ACTA IMEKO
ISSN: 2221-870X
December 2025, Volume 14, Number 4, 1 - 5

Proposal for a Si and GaAs double-junction solar cell: Characterization and simulation

Willian M. M. Bazilio[1], Rudy M. S. Kawabata[1], Guilherme M. Torelly[1], Patrícia L. de Souza[1], Daniel R. Louzada[2], Rodrigo F. Calili[2]

[1] *Department of Electrical Engineering, Pontifical Catholic University of Rio de Janeiro, Rio de Janeiro, RJ, 22451-900, Brazil*
[2] *Graduate Programme in Metrology, Pontifical Catholic University of Rio de Janeiro, Rio de Janeiro, RJ, 22451-900, Brazil*

ABSTRACT
Integrating III-V solar cells with silicon (Si) shows great promise for advancing commercial solar cell technology. Various methods exist to combine III-V and silicon, each presenting unique obstacles. Our study focuses on different III-V solar cell configurations to enhance their compatibility with silicon cells. Using the SCAPS software, we conducted simulations to design an ideal III-V device that closely aligns with commercially available Si solar cells. By optimizing the base layer's thickness and doping level during the simulations, we achieved an impressive efficiency of 25.0 %.

Section: RESEARCH PAPER

Keywords: tandem solar cell; electrical measure; III-V on Si; SCAPS simulation

Citation: W. M. M. Bazilio, R. M. S. Kawabata, G. M. Torelly, P. L. de Souza, D. R. Louzada, R. F. Calili, Proposal for a Si and GaAs double-junction solar cell: Characterization and simulation, Acta IMEKO, vol. 14 (2025) no. 4, pp. 1-5. DOI: 10.21014/actaimeko.v14i4.2030

Section Editor: Carlos Hall, PósMQI/PUC-Rio, Rio de Janeiro, Brazil

Received December 7, 2024; **In final form** October 26, 2025; **Published** December 2025

Funding: This work was supported by the National Council for Scientific and Technological Development (CNPq).

Corresponding author: Willian M. M. Bazilio, e-mail: willian.m.bazilio@aluno.puc-rio.br

1. INTRODUCTION

In solar photovoltaic energy generation, there is great interest in the development of new technologies that enhance the photovoltaic cells. This is even more important when we consider both the growing necessity for clean energy and the efficiency limits of now-a-day silicon (Si) cells. In this scenario, the coupling of III-V semiconductors and Si has been of great interest in optoelectronics, due to the potential benefits of exploiting both materials' strengths.

The combination of III-V materials with Si presents several advantages, with the main one being the fact that III-V semiconductors have a high photon absorption efficiency (due to their high crystalline quality and bandgap configuration), while Si semiconductors have low manufacturing/production costs, due to the technology's maturity and the existing large-scale production infrastructure.

The concept of photovoltaics using III-V materials on Si substrates has been known since the 1980s [1], [2]. This approach involves the use of III-V semiconductors with high crystalline quality to develop solar cells with high energy conversion efficiency. However, the production costs associated with this technology have limited its widespread use, relegating it to niche applications such as satellites.

To address the cost issue, attempts have been made to grow III-V solar cells directly on Si substrates. However, these attempts have not been very successful so far. The main challenge lies in the significant differences in lattice constants and thermal coefficients between III-V materials and Si. These differences can lead to defects and limitations in the performance of the solar cells.

Additionally, the record efficiency for Si solar cells has only improved by 0.6 % over 15 years, while III-V solar cells gained 1 % efficiency per year in the same period. Therefore, different approaches to couple III-V photovoltaic cells to silicon have attracted a lot of investment, since they have the potential to combine high efficiency with low cost.

Despite the challenges, researchers continue to explore and develop techniques to overcome the obstacles and make III-V on Si photovoltaics more viable for large-scale solar energy applications.

In this work, we chose the stacking approach to couple III-V with Si solar cells. We present the characterization results of Si solar cells produced at Pontifícia Universidade Católica do Rio

Grande do Sul (PUC-RS), and the simulation results of a III-V solar cell to be grown at Pontifícia Universidade Católica do Rio de Janeiro (PUC-Rio), which should be later stacked with the investigated Si cells.

The present work is structured as follows: the first section comprises the introduction; section 2 presents the methodology used; the results and discussions are presented in section 5; while the conclusions of the work are drawn in section 6.

2. METHODOLOGY

The work was divided into two stages: experimental testing and simulation. In the following, each of the two stages will be described in detail.

3. SIMULATION

The modelling of a hybrid solar cell consisting of an upper layer of GaAs (gallium arsenide) and a lower layer of Si was conducted. Figure 1 A) illustrates the four-terminal configuration for integrating the III-V and Si solar cells. This methodology involves the utilization of a transparent insulating adhesive to stack both cells together. Finally, the layers in the GaAs solar cell are depicted in Figure 1 B).

The top GaAs solar cell was simulated with the solar cell capacitance simulator (SCAPS) software [3], aiming to identify a suitable III-V structure to be integrated with the bottom Si solar cell. Initially, GaAs solar cells with different active layer thicknesses were analysed to assess their performance.

The software provides the *I-V* characteristics of the device, enabling the extraction of key figures of merit, including efficiency (η), short-circuit current density (I_{sc}), open-circuit voltage (V_{oc}), fill factor (FF), and maximum extracted power (P_{max}). In Table 1, the physical characteristics of the two solar cells (Si and GaAs) are presented, while Table 2 describes the electrical characteristics of each layer associated with the two solar cells, which are necessary for the simulation of electricity generation.

Given that the program's objective is to simulate a realistic solar cell, it considers not only the parameters associated with the material structure, but also various factors, such as temperature, series resistance, solar spectrum, and surface transmission. However, it is important to emphasize that the SCAPS software does not calculate surface reflection. Nevertheless, it allows users to input the spectrum for analysis.

According to the literature [4], GaAs, which possesses a 1.42 eV band gap, has been demonstrated as the optimal choice for a tandem cell with Si as the bottom sub-cell.

4. EXPERIMENTAL TESTING

For the characterization of the solar cells, an experimental setup was used consisting of a solar simulator (Sciencetech

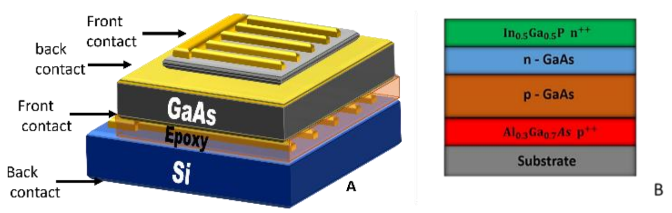

Figure 1. A) Schematic of a tandem III-V-on-Si solar cell coupled with a transparent, insulating adhesive; and B) layer structure of the GaAs cell.

Table 1. Physical properties of the two solar cells.

Solar cells	Material	Layer	Thickness in µm	Doping in cm^{-3}
Silicon	Si : N$^+$	FSF	0.03	$1{\cdot}10^{20}$
	Si : N	Front	15	$1{\cdot}10^{17}$
	Si : P	Bulk	200	$2{\cdot}10^{18}$
	Si : P$^+$	BSF	1	$1{\cdot}10^{20}$
GaAs	$In_{0.5}Ga_{0.5}P$: N^{++}	FSF	0.015	$1{\cdot}10^{19}$
	GaAs : N	Emissive	0.03	$1{\cdot}10^{19}$
	GaAs : P	Base	2550	$1{\cdot}10^{18}$
	$Al_{0.3}Ga_{0.7}As$: P^{++}	BSF	1	$1{\cdot}10^{18}$

Table 2. Electrical properties of each layer associated with the two solar cells.

Parameter	Si	GaAs	$In_{0.5}Ga_{0.5}P$	$Al_{0.3}Ga_{0.7}As$
Bandgap in eV	1120	1424	1760	1798
Electron affinity in eV	4500	4070	4090	4100
Dielectric permittivity	11900	12900	11800	11000
Electron thermal velocity in cm/s	$1{\cdot}10^{7}$	$4.4{\cdot}10^{8}$	$4.4{\cdot}10^{10}$	$3.77{\cdot}10^{8}$
Hole thermal velocity in cm/s	$1.0{\cdot}10^{7}$	$1.8{\cdot}10^{8}$	$1.8{\cdot}10^{10}$	$1.65{\cdot}10^{8}$
Electron mobility in cm^2 / (V s)	$1.5{\cdot}10^{7}$	$4.0{\cdot}10^{9}$	$8.0{\cdot}10^{5}$	$2.0{\cdot}10^{6}$
Hole mobility in cm^2 / (V s)	4.5	$5.0{\cdot}10^{4}$	$3.5{\cdot}10^{4}$	$1.38{\cdot}10^{6}$

SF300A, London, ON, Canada) and a semiconductor parameter analyser (HP 4145B, Palo Alto, CA, United States). This setup allowed the measurement of the solar cell's current density-voltage (*I-V*) characteristic curve under 1 (one) sun irradiance, facilitating the extraction of the relevant figures of merit (I_{sc}, V_{oc}, V_{oc}, P_{max}, η).

Figure 2 A) shows the Si solar cell of an area of 4.03 cm², bifacial passivated emitter rear totally diffused (PERT), in detail; and Figure 2 B) presents the cell being prepared to be tested under controlled light conditions. As the GaAs solar cell was not available, its experimental assay will be conducted on another occasion.

5. RESULTS AND DISCUSSIONS

Determining the optimal thickness of the III-V sub-cell's base layer is crucial. To achieve this, we employed the SCAPS software for simulating the photo-generated current density,

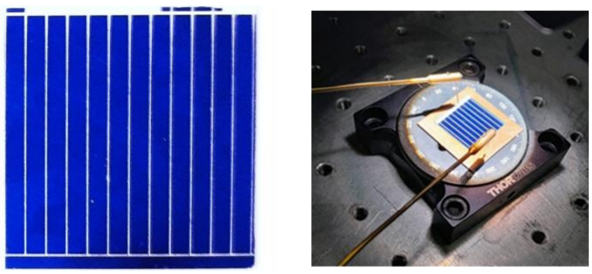

A B

Figure 2. A) Detailed view of the Si solar cell; and B) Si solar cell in the solar simulator under an irradiance of one sun.

while varying the p-base layer thickness. Figure 1 B) illustrates the schematic representation of the III-V sub-cell structure. The n-emitter layer's thickness remained constant at 0.030 μm, with doping levels of 1×10^{19} cm^{-3} and 9×10^{18} cm^{-3} for the n-emitter and p-base layers, respectively.

The simulation results are presented graphically in Figure 3. These results shed light on the impact of thickness on the figures of merit. As expected, an increase in current density is observed as the thickness ranges from 0.050 μm to 4 μm, owing to higher photon absorption. However, it is important to note that at a thickness of approximately 2.5 μm, the current density saturates. Hence, it is recommended to opt for a 2.5 μm thick base layer, which reduces material consumption, while allowing a small portion of the high-energy spectrum to be absorbed by the bottom Si sub-cell.

SCAPS provides consistent results for the electrical analysis of photovoltaic devices; however, its optical modelling is limited, as it does not account for surface reflection effects or optical coupling between sub-cells in multi-junction configurations.

For future work, it is proposed to integrate SCAPS with a complementary tool dedicated to optical calculations, in order to enhance the accuracy of the simulations.

Once the GaAs cell thickness was optimized through simulation, an experimental assay was conducted using the Si cell. The luminous intensity was varied to obtain voltage and current curves for different power levels (Figure 4).

It can be observed that, as the power is increased, the electric current becomes saturated, making it impractical to conduct a detailed analysis. To address this issue, both the short-circuit (I_{sc}) current and the open-circuit voltages (V_{oc}) were measured for different power levels, ranging from 100 W to 300 W with a step of 25 W (Figure 5 and Figure 6). In Figure 5, a linear relationship between current and power can be observed, whereas, in Figure 6, there is a linear relationship between voltage and power, albeit with a larger fitting error. The standard power for photovoltaic cell testing is the power of 300 W, or the power relative to an irradiance of 100 mW/cm^2 for an air mass (AM) of 1.5.

Figure 7 depicts the graphic of the estimated (by measure) Si current density per voltage, while Figure 8 presents the simulation of the current density per voltage.

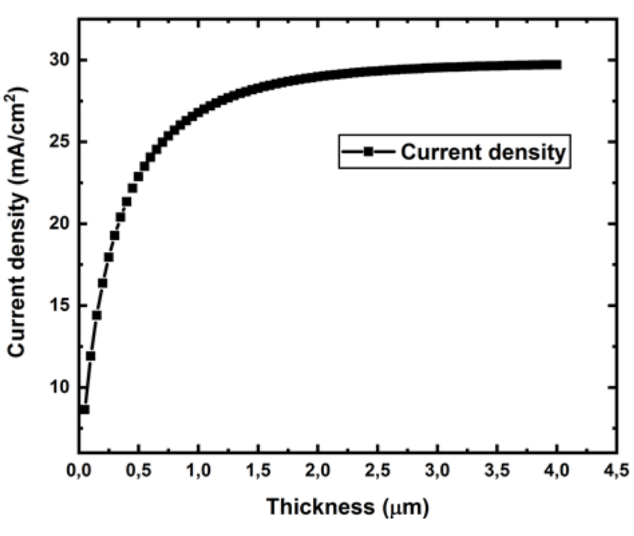

Figure 3. Current density curve as a function of the variation in base-layer thickness of a pure GaAs solar cell simulated in SCAPS, aiming to determine the thickness that maximizes the generated current.

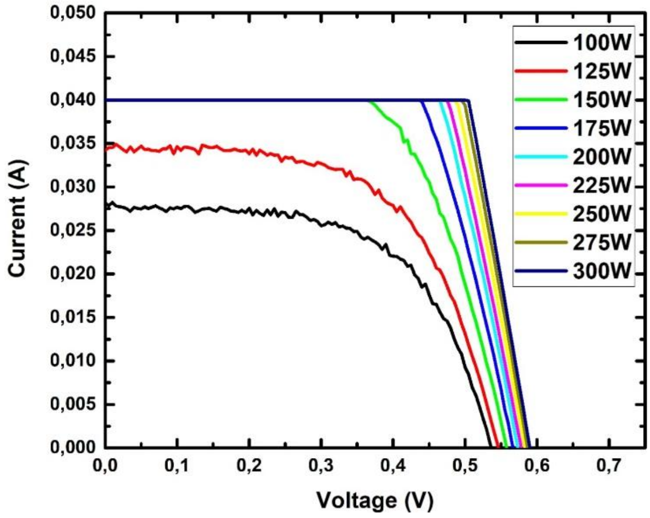

Figure 4. *I-V* curves of a silicon solar cell under varying light-source power levels of the solar simulator.

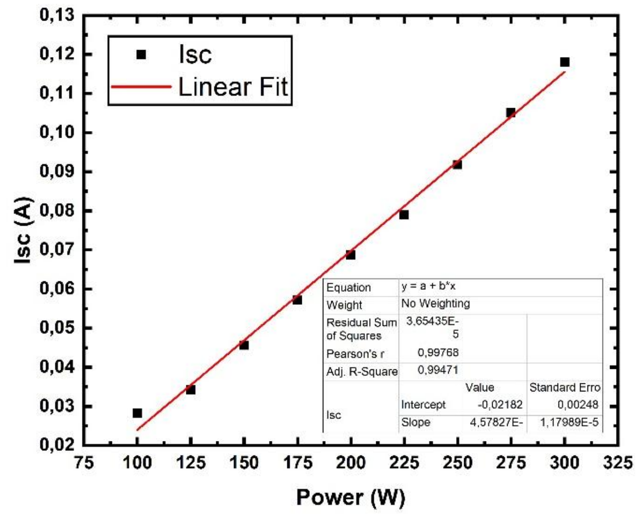

Figure 5. Linear relationship between the short-circuit current (I_{sc}) and the light-source power of the solar simulator.

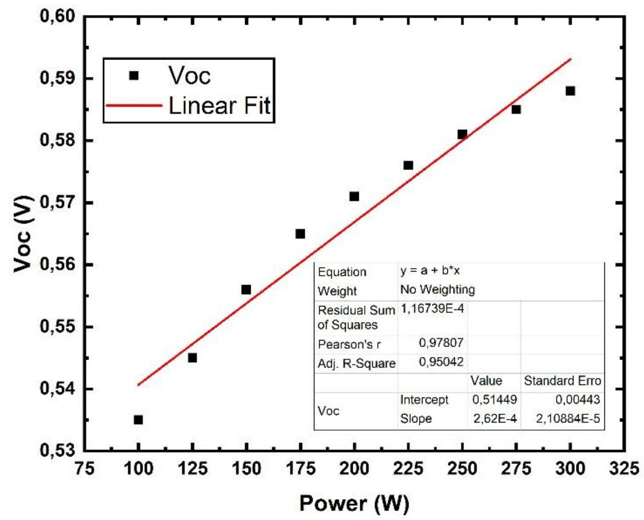

Figure 6. Linear relationship between the open-circuit voltage (V_{oc}) and the light-source power of the solar simulator

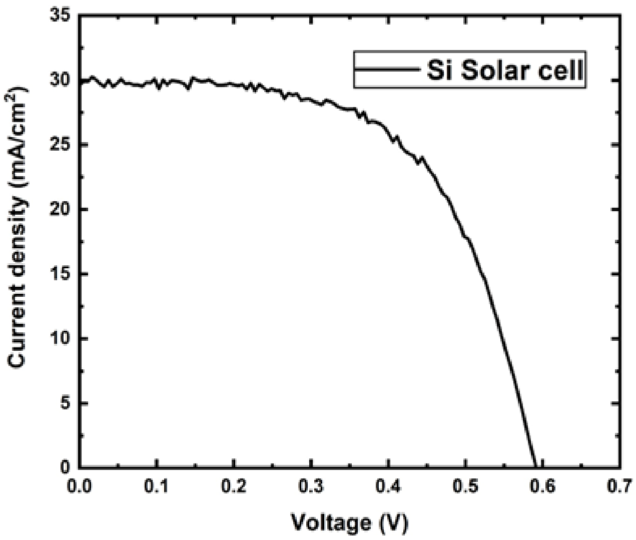

Figure 7. *I-V* curve of the silicon solar cell, estimated from the results presented in Figures 5 and 6, for a power of 300 W, equivalent to the AM1.5G spectrum.

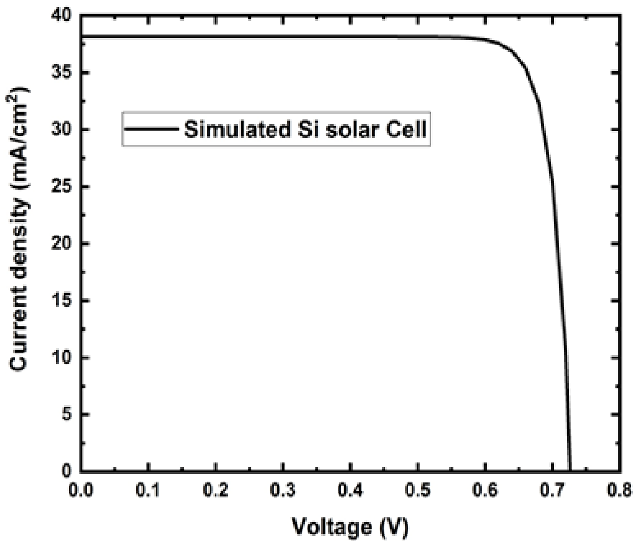

Figure 8. Simulated *I-V* curve of the silicon solar cell

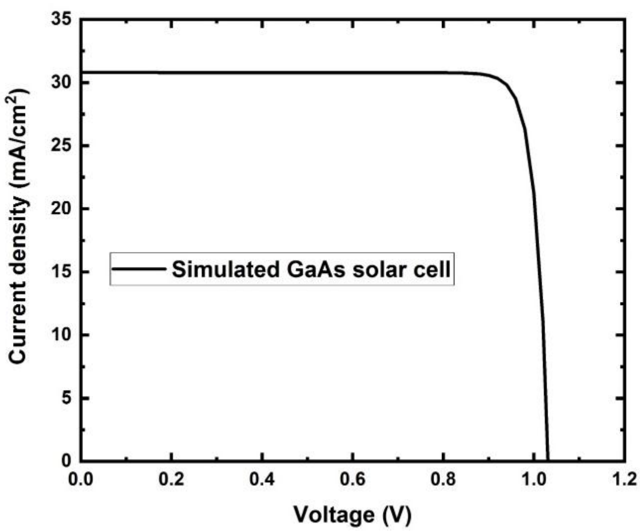

Figure 9. Simulated *I-V* curve of the GaAs solar cell showing the optimized performance at 2.5 µm base layer thickness, used to benchmark experimental results.

Table 3. Results of simulation and measured Si solar cell and the simulated GaAs solar cell.

Figure of merit	GaAs simulation	Si simulation	Si measured	Error Si %
I_{sc} in mA/cm^2	30.79	36.03	29.62	2.16
V_{oc} in V	1.03	0.62	0.59	5.10
FF in %	88.16	83.17	60.93	3.65
η in %	28.03	18.71	12.11	5.45

Figure 9 shows the simulated *I-V* curve and the figures of merit for the GaAs sub-cell with a thickness of 2.55 µm. The results obtained in the performance study of the GaAs cell regarding the base layer thickness are similar to those presented in works [5] and [6]. In Table 3, a summary of the figures of merit obtained through simulation and measurement is presented.

6. CONCLUSION

GaAs have been investigated as a Si tandem partner for a silicon solar cell. Simulation results indicate that a 2.5 µm thick GaAs p-type base layer should be used in the III-V sub-cell in a stacked configuration with Si as the bottom device. For future work aiming for better coupling, simulations will be conducted with different emitter thicknesses and other III-V materials, such as InGaP (indium gallium phosphide), which has a higher energy gap than GaAs. The intention to simulate these materials is justified considering a better absorption of higher-energy photons, resulting in a higher I_{SC}. We will also simulate the complete structure in order to estimate the combined efficiency and compare it with that of the individual Si cell.

AUTHORS' CONTRIBUTION

Rudy Kawabata contributed to the assembly of the experimental setup and the execution of electrical measurements. Guilherme Torelly, Patricia Lustoza, Daniel Louzada, and Rodrigo Calili were played a key role in the discussions of the results and in writing the text.

ACKNOWLEDGEMENT

This work was carried out with the support of the Coordination for the Improvement of Higher Education Personnel (CAPES) - Financing Code 001.

REFERENCES

[1] J. M. Gee, G. F. Virshup, A 31%-efficient GaAs/silicon mechanically stacked, multijunction concentrator solar cell, Conference Record of the Twentieth IEEE Photovoltaic Specialists Conference, vol. 1 (1988), pp. 754-758.
DOI: 10.1109/PVSC.1988.105803

[2] N. Jain, M. K. Hudait, III–V Multijunction Solar Cell Integration with Silicon: Present Status, Challenges and Future Outlook, Energy Harvesting and Systems, vol. 1 (2014) no. 3-4, pp. 121-145.
DOI: [10.1515/ehs-2014-0012](10.1515/ehs-2014-0012)

[3] M. Burgelman, K. Decock, J. Verschraegen, A. Niemegeers, S. Degrave, SCAPS-1D (version 3.8). Online [Accessed 15 March 2023]
https://scaps.elis.ugent.be

[4] Z. J. Yu, M. Leilaeiounet, Z. Holman, Selecting tandem partners for silicon solar cells, Nature Energy, Solar Energy, 1 (2016) 16137, pp. 8-9.
DOI: 10.1038/nenergy.2016.137

[5] T. Borrely, A. A. Quivy, Realistic Simulations and Design of GaAs Solar Cells produced by Molecular Beam Epitaxy, 34th Symposium on Microelectronics Technology and Devices (SBMicro), São Paulo, Brazil, 26-30 August 2019, pp. 1-4. DOI: [10.1109/SBMicro.2019.8919412](https://doi.org/10.1109/SBMicro.2019.8919412)

[6] F. D. Silva, D. N. Micha, High-Efficiency GaAs Solar Cell Optimization by Theoretical Simulation, 34th Symposium on Microelectronics Technology and Devices (SBMicro), São Paulo, Brazil, 26-30 August 2019, pp. 1-4. DOI: [10.1109/SBMicro.2019.8919411](https://doi.org/10.1109/SBMicro.2019.8919411)